AIP | Review of Scientific Instruments

Versatile single-molecule multi-color excitation and detection fluorescence setup for studying biomolecular dynamics

M. A. Sobhy, M. M. Elshenawy, M. Takahashi, B. H. Whitman, N. G. Walter et al.

Citation: Rev. Sci. Instrum. **82**, 113702 (2011); doi: 10.1063/1.3657153
View online: http://dx.doi.org/10.1063/1.3657153
View Table of Contents: http://rsi.aip.org/resource/1/RSINAK/v82/i11
Published by the AIP Publishing LLC.

Additional information on Rev. Sci. Instrum.

Journal Homepage: http://rsi.aip.org
Journal Information: http://rsi.aip.org/about/about_the_journal
Top downloads: http://rsi.aip.org/features/most_downloaded
Information for Authors: http://rsi.aip.org/authors

ADVERTISEMENT

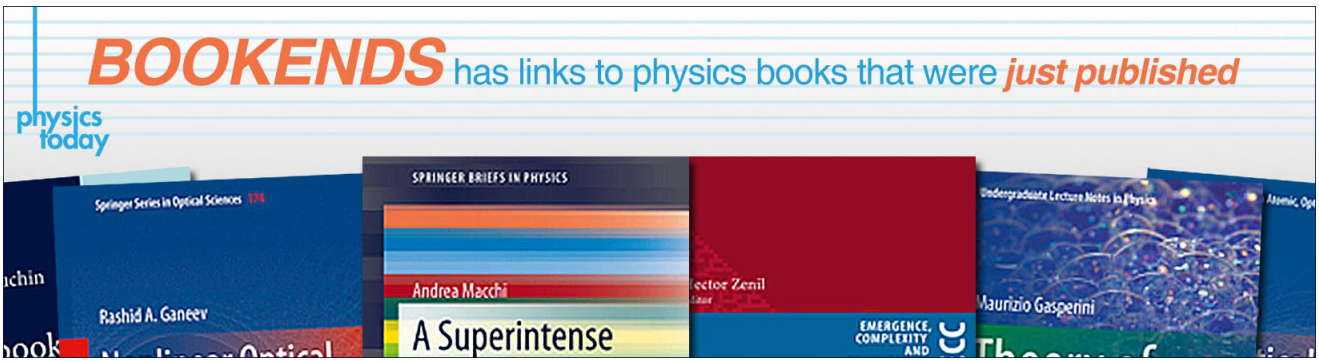

Downloaded 28 Jun 2013 to 141.211.173.82. This article is copyrighted as indicated in the abstract. Reuse of AIP content is subject to the terms at: http://rsi.aip.org/about/rights_and_permissions

Versatile single-molecule multi-color excitation and detection fluorescence setup for studying biomolecular dynamics

M. A. Sobhy,[1] M. M. Elshenawy,[1,a)] M. Takahashi,[1] B. H. Whitman,[2] N. G. Walter,[3] and S. M. Hamdan[1,b)]

[1]*Laboratory of DNA Replication and Recombination, Division of Chemical and Life Sciences and Engineering, King Abdullah University of Science and Technology, Thuwal 23955, Saudi Arabia*
[2]*Laser Launch LLC, York, Pennsylvania 17403, USA*
[3]*Department of Chemistry, Single-Molecule Analysis Group, University of Michigan, Ann Arbor, Michigan 48109, USA*

(Received 5 July 2011; accepted 6 October 2011; published online 7 November 2011)

Single-molecule fluorescence imaging is at the forefront of tools applied to study biomolecular dynamics both *in vitro* and *in vivo*. The ability of the single-molecule fluorescence microscope to conduct simultaneous multi-color excitation and detection is a key experimental feature that is under continuous development. In this paper, we describe in detail the design and the construction of a sophisticated and versatile multi-color excitation and emission fluorescence instrument for studying biomolecular dynamics at the single-molecule level. The setup is novel, economical and compact, where two inverted microscopes share a laser combiner module with six individual laser sources that extend from 400 to 640 nm. Nonetheless, each microscope can independently and in a flexible manner select the combinations, sequences, and intensities of the excitation wavelengths. This high flexibility is achieved by the replacement of conventional mechanical shutters with acousto-optic tunable filter (AOTF). The use of AOTF provides major advancement by controlling the intensities, duration, and selection of up to eight different wavelengths with microsecond alternation time in a transparent and easy manner for the end user. To our knowledge this is the first time AOTF is applied to wide-field total internal reflection fluorescence (TIRF) microscopy even though it has been commonly used in multi-wavelength confocal microscopy. The laser outputs from the combiner module are coupled to the microscopes by two sets of four single-mode optic fibers in order to allow for the optimization of the TIRF angle for each wavelength independently. The emission is split into two or four spectral channels to allow for the simultaneous detection of up to four different fluorophores of wide selection and using many possible excitation and photoactivation schemes. We demonstrate the performance of this new setup by conducting two-color alternating excitation single-molecule fluorescence resonance energy transfer (FRET) and a technically challenging four-color FRET experiments on doubly labeled duplex DNA and quadruple-labeled Holliday junction, respectively. © *2011 American Institute of Physics*. [doi:10.1063/1.3657153]

I. INTRODUCTION

The multidisciplinary approach of combining biochemical, biophysical, and structural tools has successfully addressed many biological problems at the molecular level.[1] Nonetheless, the ensemble averaging associated with biochemical methods and the static nature of the images provided by structural techniques limit us in understanding the dynamic behavior of biomolecules and the nature of their interactions.[2] Single-molecule techniques provide the missing component in this multidisciplinary approach by allowing to track each molecule and to record molecular movies of biological reactions.[3] Single-molecule experimental approaches are currently expanding with the application of wide range of force and fluorescence microscopy techniques to study individual molecules both *in vitro* and *in vivo* with high spatial and temporal resolution.[4]

Total internal reflection fluorescence (TIRF) and fluorescence resonance energy transfer (FRET) are key concepts applied in single-molecule fluorescence imaging. TIRF enables the imaging of single fluorophores by suppressing the fluorescence background from solution through restricting the depth of illumination to an evanescent wave layer of about 100 nm above the surface of the cover slip.[5] FRET measures the radiationless energy transfer between donor and acceptor molecules and thus provides a molecular ruler that can measure the inter- and/or intramolecular distances in the range of 2–8 nm.[6,7] Single-molecule TIRF and FRET microscopy have proven their novelty in studying the distributions and the fluctuations of biomolecules and elucidating their reaction mechanisms by observing short-lived transient intermediary steps including conformational changes and dynamic interactions as well as building the timing mechanism of the steps by which biomolecules mediate their activities.[8]

A key feature of the single-molecule TIRF and FRET experiment is the ability to conduct simultaneous multi-color excitation and detection of single-molecule fluorophores with high spatial and temporal resolution. The development

a)Graduate Program in Biosciences.
b)Author to whom correspondence should be addressed. Electronic mail: samir.hamdan@kaust.edu.sa.

 © 2011 American Institute of Physics

Downloaded 28 Jun 2013 to 141.211.173.82. This article is copyrighted as indicated in the abstract. Reuse of AIP content is subject to the terms at: http://rsi.aip.org/about/rights_and_permissions

of this feature is critical to the future advancement of single-molecule fluorescence imaging particularly in two directions: studying biological processes that are mediated by multi-protein complexes[9] and achieving sub-diffraction limit resolution.[10] Large multi-protein complexes mediate highly coordinated activities and thus require the simultaneous detection of more observables at a time.[11] Super resolution techniques rely on fluorophores that can be selectively switched on "bright" and off "dark" to allow the detection of few molecules at a time.[12] This requires the use of a sequence of excitation wavelengths for controlled durations or illumination using multiple wavelengths, as well as adjusting the intensities of each wavelength. Most current objective-based single-molecule TIRF setups use free space coupling of all the laser lines through the back port of the microscope. The combined laser beam is then expanded by a telescope to fill the back focal plane of the objective. The incidence angle of the beam is adjusted by changing the position of a collimating lens that directs the beam off-axis and achieves TIRF. Hence TIR angle is wavelength dependent, free space coupling cannot achieve equal penetration depth of individual wavelengths into the sample. Furthermore, it also requires frequent adjustments and hands-on experience from the user. Coupling individual excitation lasers via optics-fibers, on the other hand, will enable the independent control of the TIR angle. The introduction of the 1.4 numerical aperture (NA) oil-immersion objectives has largely solved the high background problem associated with objective-based TIRF in the past. The signal-to-noise ratio of the single and two-color single-molecule FRET data is indistinguishable between objective-based TIRF and prism-based TIRF.[2] Nonetheless prism-based TIRF is more favorable in multi-color applications since it does not require the multi-band dichroic mirror associated with the objective-based TIRF, which cuts out a significant fraction of the emission light. We applied objective-based TIRF because of its better integration with optic-fibers and its compatibility with the motorized controllers of the optic-fibers to achieve reproducibility in individual TIR angles and ease in identifying the coincidence of the multi-color excitation sources on the sample. The alternation between different excitation wavelengths in most of the current TIRF setups is accomplished by utilizing mechanical shutters. For example, in a recent study Lee *et al*. measured FRET between four different fluorophores by three-color excitation TIRF using shutters, electronic flip-flop and multiplexer circuits.[13] A similar approach was implemented to achieve fast alternation between multiple wavelengths in super-resolution techniques (PALM,[14] FPALM,[15] and STORM[16]). Mechanical shutters rely on movable parts, require few to tens of milliseconds to open and close and produce high noise particularly when several units are used to control multiple laser sources. They also cannot control the laser power and therefore are commonly combined with neutral density filters to reduce the laser power. Furthermore, the driver modules for mechanical shutters control three or four shutters at a time. On the other hand, AOTFs do not involve any moving components or noise and rely on changing the refractive index of a nonlinear crystal due to oscillating electric fields of different frequencies. Typically AOTFs can control eight wavelengths simultaneously in addition to their excellent pointing stability, high extinction ratio and maintaining the beam quality. The driver module can control up to 16 channels. Furthermore, the laser intensities for individual wavelengths can be controlled by adjusting the amplitude of the electric field signal. Finally, the crystals of the AOTFs can stand high power densities and have long lifetime. AOTFs are typically used in multiple wavelengths confocal microscopes but to our knowledge this is the first time they are used in wide-field TIRF microscopy.

In this paper, we present in detail the design and construction of a custom-built objective-type TIRF setup that is optimized for simultaneous and alternating multi-color excitation and detection of single-molecule fluorophores. The setup can be used for measuring FRET between multiple fluorophores and multi-color single-particle tracking using any combination of up to seven different wavelengths. The laser sources are equally accessible and efficiently shared between two microscopes through a compact laser combiner module. Each microscope can transparently and independently control the wavelength selection process through its own AOTF without compromising the range of wavelength selection or the need to duplicate the laser sources. The individual AOTFs in the combiner provide fully programmable alternation and multiplexed excitation schemes with switching time on the order of few microseconds compared to millisecond range in mechanical shutters. It should be noted that despite this fast alternation time, this feature of the AOTF is limited by the milliseconds exposure time of the electron-multiplied CCD (EMCCD) camera. The laser combiner has two identical sets of four optic fibers outputs, one set for each microscope. Optic fibers have pre-focused and integrated optical assemblies and therefore provide excellent beam pointing stability for precision measurements. More importantly, coupling individual laser lines into the microscope through separate optic fibers allows the independent control of the TIR angle and penetration depth for each wavelength. The synergy between the laser combiner and using individual optic fibers allows the detection of up to four different spectral channels with a wide selection of fluorophores and using many possible excitation and photoactivation schemes.

II. DESCRIPTION

The design of the single-molecule TIRF setup is based on sharing multi-color laser combiner module between two motorized inverted fluorescence microscopes. The setup configuration is well-integrated, highly compact, cost-effective and provides flexibility in sharing, selecting and controlling the intensities of the multiple laser wavelengths. The setup is mounted on actively damped vibration-isolation pneumatic SmartTable® from Newport (M-OTS-ST-410-12I) to isolate the setup from the building vibrations and to minimize the mechanical drifts. The entire setup is placed inside a freestanding custom enclosure from Newport of dimensions (125 in. L × 48.5 in. W × 72 in. H) with clear acrylic sliding panels to provide contained environment for the setup and the optical components (Figure 1). The enclosure has a clean air blower with a filter assembly to maintain uniform air flow. The enclosure is then surrounded by a lightproof curtain made

Downloaded 28 Jun 2013 to 141.211.173.82. This article is copyrighted as indicated in the abstract. Reuse of AIP content is subject to the terms at: http://rsi.aip.org/about/rights_and_permissions

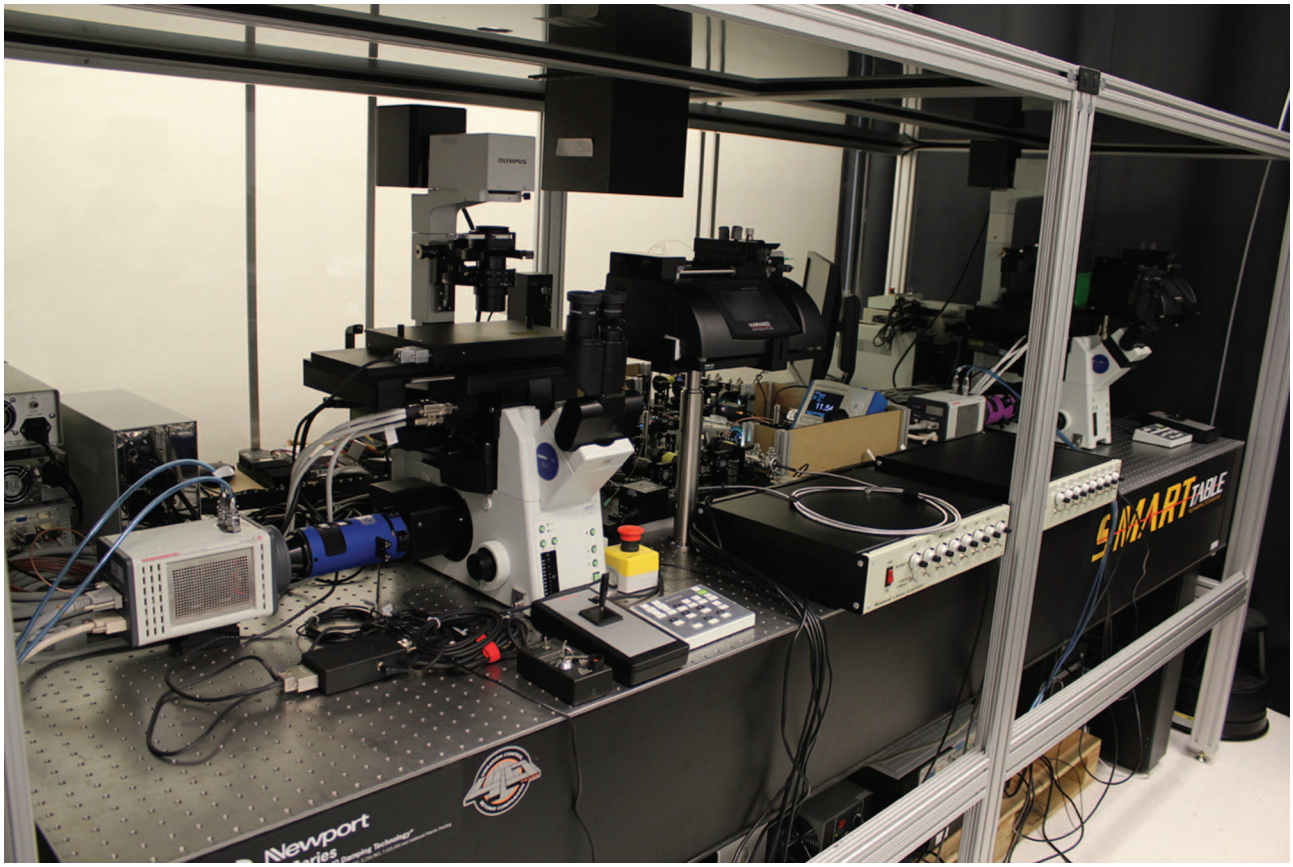

FIG. 1. (Color) Photo of the single-molecule TIRF setup showing the two motorized inverted microscopes with linear encoded stages, the laser combiner module and two manual controllers in the middle, the EMCCD detectors, the controllers for the microscopes and the peripherals. The fluorescence setup is mounted on actively damped vibration-isolation SmartTable® (Newport) and surrounded with an enclosure with transparent acrylic panels. The air in the room is temperature-controlled and is filtered through a HEPA filter unit. A lightproof regular duty laser curtain (Kentek) surrounds the single-molecule fluorescence setup. (The front panels of the enclosure are taken out for the photo.)

of black Kentek FLEX-GUARD™ regular duty laser curtain. The illumination in the room is controlled with two separate electric circuits, one for the lights inside the dark curtain and another for the outer lights. The temperature in the room is controlled with a thermostat and the air is filtered through a high-efficiency particulate air (HEPA) filter with adjustable air flow speed.

The multi-color laser combiner (Figure 2(a)) contains a total of six laser sources that span across the visible range from 400 to 640 nm, which provides flexibility in choosing the fluorophore that is most suited for the biomolecular process under study. There are five solid-state lasers from (Coherent Inc.), which are rated for 100 mW output power and have circular beam profile. The wavelengths of these lasers are 405 nm (Cube 405-100-C), 488 nm (Sapphire 488-100 CW CDRH), 532 nm (Compass 315M-100), 561 nm (Sapphire 561-100 CW CDRH), and 640 nm (Cube 640 100C). The laser heads are mounted on aluminum blocks that act as a heat sink and provide the appropriate and equal height for the laser beams. The dimensions for the Cube mounts are (4 in. L × 2 in. W × 1–7/16 in. H) and those for the Sapphire laser mounts are (4–15/16 in. L × 3 in. W × 1–7/16 in. H). The base of the combiner is made of a black anodized aluminum breadboard from (Thorlabs, NJ, USA). The sixth laser is an argon laser (Stellar Pro-L) from (Modu-Laser, UT, USA), which is coupled to the combiner through a single-mode optic fiber at the position next to the Sapphire 488 nm laser head from the left side as shown in Figure 2(a). The argon laser is rated at 300 mW maximum output power and emits, besides the 488 nm, both 457 and 514 nm for the excitation of cyan fluorescent protein (CFP) and yellow fluorescent protein (YFP), respectively. Both the laser head and the power supply of the argon laser are contained in one unit, which is placed under the vibration-isolation table in order to avoid the generated heat and the vibrations from the cooling fans. The combiner, as seen in the schematic in Figure 2(a), has two symmetric sets of outputs for coupling four optic fibers to each microscope. The wavelengths outputs prior to the optic fibers on each set are controlled by an AOTF (Gooch & Housego TF527-245-6-3-GH18). The wavelengths and the intensities of the individual lines can be selected by tuning the drive frequency on an eight channels AOTF programmable driver (Gooch & Housego MSD040-150-0.2ADM-A5H-8X1). Each microscope can remotely control its designated AOTF driver using either a real-time controller in the microscope PC or an eight-channel/16-bit analog output board (PCI-DDA08/16) from (Measurement Computing Corporation, MA, USA) installed inside a Dell T7500 workstation. The output from each analog board is connected via a 100-pin cable to a break-out box and then is rewired to provide the

Downloaded 28 Jun 2013 to 141.211.173.82. This article is copyrighted as indicated in the abstract. Reuse of AIP content is subject to the terms at: http://rsi.aip.org/about/rights_and_permissions

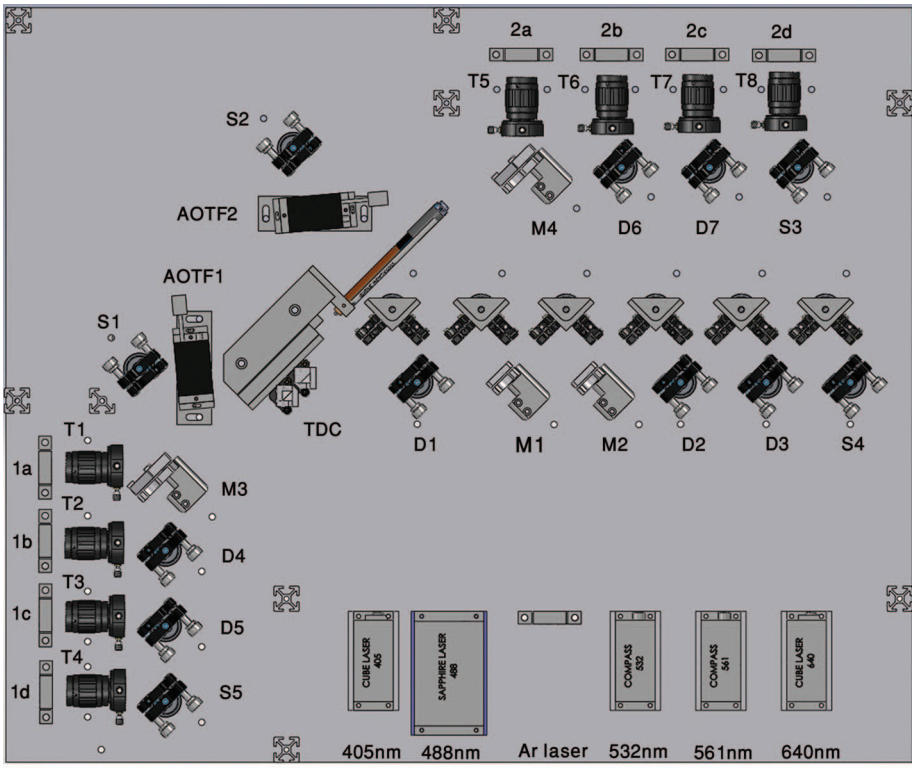

(a)

(b)

FIG. 2. (Color) (a) Schematic diagram of the laser combiner module showing the main components: (1) Solid-state laser heads from left to right are 405, 488, fiber connector for the argon laser, 532, 561, and 640 nm. The optics combining the lasers are LM01-427-25, LM01-503-25, FF520-Di02-25, LM01-552-25, LM01-613-25 and 100% reflective mirror, respectively. (2) Two AOTFs (AOTF1, 2) and two symmetric sets of four fiber outputs 1a–d and 2a–d. The Kinematix fiber manipulators are attached to the holders where band-pass clean-up filters are mounted. M1–M4 are motorized mounts, TDC = power supply for DC micrometer-actuator for the beam splitter cube and reflector prism, S1–S5 are silver mirrors, D1–D7 are dichroic mirrors, and T1–T8 are telescopes. (b) Photo of the actual laser combiner showing the laser combiner components depicted in Figure 2(a), the top lightproof cover was taken out for the photo.

respective AOTF synthesized frequency driver with a parallel port interface. Each laser beam is reflected off the surface of two 0.5 in. (12.5 mm) diameter beam-steering mirrors (BB05-E02) from Thorlabs, which are fixed at a right angle with respect to each other (Figure 2(a)). The dichroic mirrors and the band-pass filters in the following description are from (Semrock Inc.) unless otherwise noted. The single-mode optic fibers (KineFLEX-P-3-S-405-640-0.7-FCP8-P2) and fiber manipulators are from (Qioptiq). The motorized flipping mounts are from New Focus (model 8892) and are remotely

Downloaded 28 Jun 2013 to 141.211.173.82. This article is copyrighted as indicated in the abstract. Reuse of AIP content is subject to the terms at: http://rsi.aip.org/about/rights_and_permissions

controlled by external switches. The output from Laser 1 (405 nm) is reflected off the surface of two 0.5 in. steering mirrors then reflected by a dichroic mirror D1 (LM01-427-25) (Figure 2(a)). After passing through AOTFs 1 and/or 2, the 405 nm beam is decoupled through two dichroic mirrors (LM01-427-25) mounted in motorized flipping mounts M3 and M4, which are in front of the outputs of fibers 1a and 2a, respectively (Figure 2(a)). The flipping mount has a custom-made holder that carries a 100% reflective mirror besides the dichroic mirror such that at the first position the 405 nm is coupled into optic fibers 1a and/or 2a and at the second position all the wavelengths are directed into these fibers. The motorized mount offers high stability and repeatability in the beam position necessary for the efficient coupling of the laser beam into the optic fiber. There is a clean-up filter (Edmund Optics P65-133 405/10 nm) mounted on each of the holders to which the Kinematix® fiber manipulators for fibers 1a and 2a are attached.

Laser 2 (Sapphire 488 nm) is reflected by a dichroic mirror (LM01-503-25) that is mounted in a motorized flipping mount M1 (Figure 2(a)). After passing through the AOTFs, the 488 nm is coupled into optic fibers 1b and 2b by two single-edge dichroic beam splitters, D4 and D6 (FF495-Di03-25), respectively, and passes through (FF02-460/80-25) band-pass clean-up filters that are mounted in the optic fiber manipulator holders. Laser 3 is the fiber coupled multiline argon laser that emits 457, 488, and 514 nm and its output is reflected by a (FF520-Di02-25) dichroic beam splitter, which is mounted in a motorized flipping holder M2 (Figure 2(a)). In order to use the wavelengths from the argon laser, the dichroic mirror in front of Laser 2 is flipped down to move out of the beam path, while the dichroic mirror in front of the argon laser fiber is placed in the beam path. The 457 and 488 nm lines from the argon laser are coupled into optic fibers 1b and/or 2b by dichroic mirrors D4 and D6, respectively. The 514 nm line is directed into fibers 1c and/or 2c by dichroic mirrors D5 and D7 (LM01-552-25), respectively, and then passes through (FF01-525/45-25) band-pass clean-up filters (Figure 2(a)). To use the output from the Sapphire 488 nm laser along with the 514 nm, both dichroic mirrors in front of Lasers 2 and 3 are placed in the beam path. The output from Laser 4 (532 nm) is reflected by the dichroic beam splitter D2 (LM01-552-25) and directed into optic fibers 1c and/or 2c by dichroic beam splitters D5 and D7 (LM01-552-25), respectively, after passing through (FF01-525/45-25) clean-up filters. Laser 5 (Sapphire 561 nm) and Laser 6 (640 nm) are reflected by dichroic beam splitter D3 (LM01-613-25) and 100% reflective mirror S4, respectively, before going through the AOTFs. Both 561 and 640 nm are directed into optic fibers 1d and 2d by 100% reflective mirrors S5 and S3, respectively, and pass through Edmund Optics Precession long-pass 550 (P62-984) band-pass filters in the fiber manipulator holder. The collinear laser beams reflected by the afore-mentioned dichroic mirrors are directed into AOTFs 1 and 2, by reflective mirrors S1 and S2, respectively (Figure 2(a)). The laser can be either split equally between the two AOTFs or directed into either AOTF 1 or 2 using a 50:50 non-polarizing beam splitter cube (BS010) or a right angle prism (PS910H-A) with antireflection coating from Thorlabs, respectively (Figure 2(a)). Both the prism and the beam splitter are mounted on a custom-made aluminum piece and their position is precisely controlled by a PC-controlled dc servo motor actuator with 25 mm travel (Z825B) and (TDC001) power supply from Thorlabs to achieve reproducible positioning and to maintain the alignment of the laser beam into the optic fibers. The output from each AOTF is separated into four different lines (fiber 1: 405 nm, fiber 2: 457 and 488 nm, fiber 3: 514 and 532 nm, and fiber 4: 561 and 640 nm), which are coupled into the microscopes through individual optic fibers (Figure 2(a)). Also all the wavelengths can be directed into fibers 1a and/or 2a by the 100% reflective mirrors in the motorized mounts in front of these fibers. The laser beams diverge along their optical path to an extent that varies depending on the wavelength and the laser source type. This divergence causes the laser beam size to increase beyond the optimum diameter (0.7 mm) for coupling into the single-mode optic fibers, which results in severe loss of the output power from the optic fiber. In order to collimate the laser beams down to the appropriate size for the optic fiber, we placed telescopes of different magnifications (2×, 2.77×, and 3.3×) before the optic fibers. The telescopes helped tremendously in the case where the same optic fiber is used to transmit lasers of different wavelengths and also to achieve maximum transmission efficiency in the fibers transmitting individual wavelengths. The telescopes are made of concave and convex achromatic doublet lenses with visible range 400–700 coating, where the flat sides of both lenses are placed facing each other and towards the inside of the tube. The concave lens is located at the fiber side while the convex lens faces the 45° angle dichroic mirror. The two lenses are placed apart at the sum of their focal lengths, which is selected to be around 1 in. in length. The tube of the telescope is made of Thorlabs SM1NR05 zoom housing which provides 18 mm of linear travel to accurately control the focusing of the laser beam into the fiber. Each telescope is attached to XY translational mount Thorlabs LM1XY. The 2, 2.77, and 3.3× telescopes (T1–T8) (Figure 2(a)) use f = 50 mm achromatic doublet AC-127-050-A (12.5 mm diameter) positive lens. The 2× telescope uses ACN127-25-A f = –25 mm plano concave lens. The 2.77 × telescope uses f = –18 mm plano concave lens LC2873-A with LMRA9 adapter. The 3.3× telescope uses f = –15 mm plano concave LC2265-A (12.5 mm diameter). The photo of the laser combiner without the top lightproof cover showing the aforementioned components is shown in Figure 2(b).

The control diagram of the combiner and the electrical connections layout are depicted in Figure 3. Each microscope selects the wavelength combinations and the intensities of individual wavelengths by custom routines, which control the eight-channel/16-bit analog output board. The control board supplies analog signals to the individual channels in the respective AOTF frequency driver. Alternatively, the wavelengths selection and intensities can be controlled by manual controllers that adjust the intensities of individual laser lines or a real-time board in the computer that control the motorized microscope. The AOTF is a solid-state, electronically tunable band-pass filter with high extinction ratio, i.e., the ratio between the maximum and the minimum light intensity of the beam when the AOTF is in "open" or in "closed"

Downloaded 28 Jun 2013 to 141.211.173.82. This article is copyrighted as indicated in the abstract. Reuse of AIP content is subject to the terms at: http://rsi.aip.org/about/rights_and_permissions

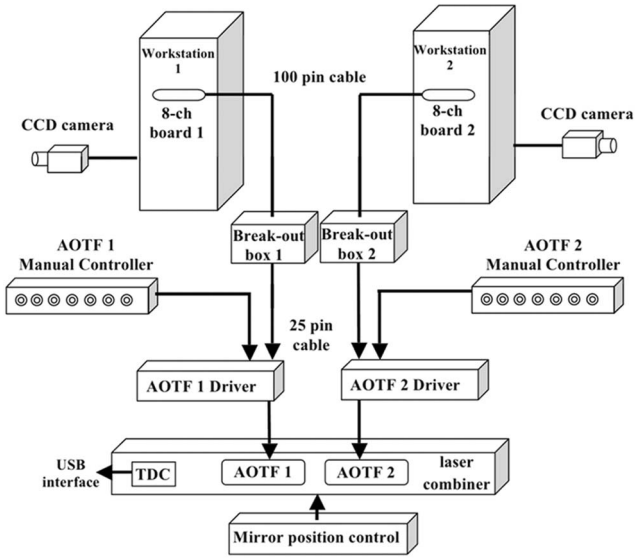

FIG. 3. The control diagram and electrical connections layout for controlling the laser combiner on each microscope. Each eight-channel/16-bit analog output board is installed in a Dell T7500 workstation. The board is connected with a 100 pin cable to a break-out box where the cable is rewired to make a 25 pin parallel port interface connected to the respective AOTF synthesized frequency driver. Alternatively a manual controller can control the AOTF driver through individual knobs that adjust the intensities of individual wavelengths. The TDC power supply for the micrometer-actuator is controlled by one workstation and each computer is connected to a Scion CFW-1612M fire wire camera that can be attached to the microscope via dual camera port.

position. To ensure that this feature does not limit its use in TIRF single-molecule fluorescence setups, we measured the extinction ratio of the AOTF at each wavelength and found it to be between 149:1 and 647:1 depending on the wavelength. Consequently, at the few milliwatts power required to excite fluorophores in single-molecule fluorescence experiments, only few microwatts of residual light are transmitted through the AOTF when it is in "closed" position. Furthermore, at the TIRF angle we could not detect any light from the objective when the AOTF is in "closed" position. Finally, even in highly sensitive single-molecule fluorescence experiment, such as FRET, we found that the FRET value to be unaffected demonstrating that the emission and the notch filters used in our setup can effectively block the residual light from the AOTF when it is in "closed" position. The AOTF driver module provides the RF signals required by the AOTF crystal to select and control the amplitude of different wavelengths. The driver unit (Gooch & Housego MSD040-150-0.2ADM-A5H-8X1) inside this module is connected to a 24 V dc power supply Triad model AWSP40-24. The module has an electric fan to remove the generated heat from the driver unit and a parallel port interface to connect the unit to the manual controller or the eight-channel/16-bit analog output board as mentioned above. The combination of individual wavelengths can also be controlled by transistor-transistor logic signals supplied by BNC connectors in the real-time controller in the PC that controls the microscope. The schematics of the manual controller for the AOTF are shown in Figure 4, which has a 5 V dc power supply and 10 kΩ variable resistors to control the amplitude of the individual lines and consequently the laser intensity of the respective wavelength. The wiring of the parallel port interface was made to correspond to the pin-assignment of the AOTF driver unit from the AOTF manufacturer.

The microscopes are two IX81 motorized inverted microscopes from Olympus with integrated zero-drift compensation system that uses an infrared laser diode (785 nm) and a photodetector for the compensation of focus drift and shift. Each microscope is controlled with its own PC computer running Cell^R® software (Olympus). The epifluorescence illumination system is coupled to the microscope through an optic fiber and has an intensity attenuator and shutter with 1 ms on/off time. The illumination source is a Mercury-Xenon 150 W short arc burner and 8-position excitation filter wheel for 25 mm filters. The epifluorescence filter sets for the two microscopes and the fluorophores that are commonly used with each set are listed in Table I. The transmitted illumination is provided through a halogen lamp where the light is collimated through a long working distance condenser. We use phase contrast rings with the 10, 20, and 40× Universal Plan Fluorite objectives and Differential Interference Contrast (DIC) with the Apochromatic TIRF 60 and 100× (NA 1.49) objectives. Each microscope has a linear encoded motorized stage (Märzhäuser) for high accuracy and reproducibility in tracking fluorophores. The first microscope has a motorized TIRF illumination combiner with four laser fiber ports with single-point bleaching optics for the 405 nm laser and a back port for wide-field illumination. The mirrors on the four lines TIRF are 430 long-pass, 500 long-pass, 525/50 band-pass, and a 100% reflective mirror to match the fiber output dichroics in the laser combiner (Figure 2(a)). Thus the wavelengths at the four ports of the microscope are: Port 1: 405 nm, Port 2: 457 and 488 nm, Port 3: 514 and 532 nm, and Port 4: 561 and 640 nm. This microscope has a piezo stage (NanoscanZ) from (Prior Scientific) with nanometer resolution and 100 μm range. The positions of the individual fibers in the four-line TIRF system are motorized and controlled by the Cell^R® software for reproducible adjustment of the TIRF angles and penetration depth for each wavelength. The second microscope currently has a single-line TIRF and a port for wide-field epifluorescence. The excitation laser wavelengths are coupled into the optic fiber using 2× telescope. The future upgrade from single to four-line illuminator is taken into account in the design of the laser combiner module. On the emission side of the single-line microscope, there is a motorized 8-position 25 mm filter wheel that is directly attached to the side port of the microscope then a Dualview, two-channel emission device (Photometrics, AZ, USA), which is coupled to a 512 × 512 EMCCD camera (Hamamatsu C9100-13) with on-chip amplification. The detection of single-molecules and the minimization of dark current to a negligible level are achieved by deep cooling of the EMCCD camera till –80 °C using water bath circulator Julabo F25-ED. The flow rate is adjusted to 1.2 l/min for each camera. Similarly the four-line system has a motorized emission filter wheel, a Quadview, a four-channel emission device (Photometrics) for performing four-color FRET experiments, besides a spare Dualview for two-color FRET measurements and a Hamamatsu C9100-13 EMCCD camera. The emission filters and dichroic beam splitters that are used

Downloaded 28 Jun 2013 to 141.211.173.82. This article is copyrighted as indicated in the abstract. Reuse of AIP content is subject to the terms at: http://rsi.aip.org/about/rights_and_permissions

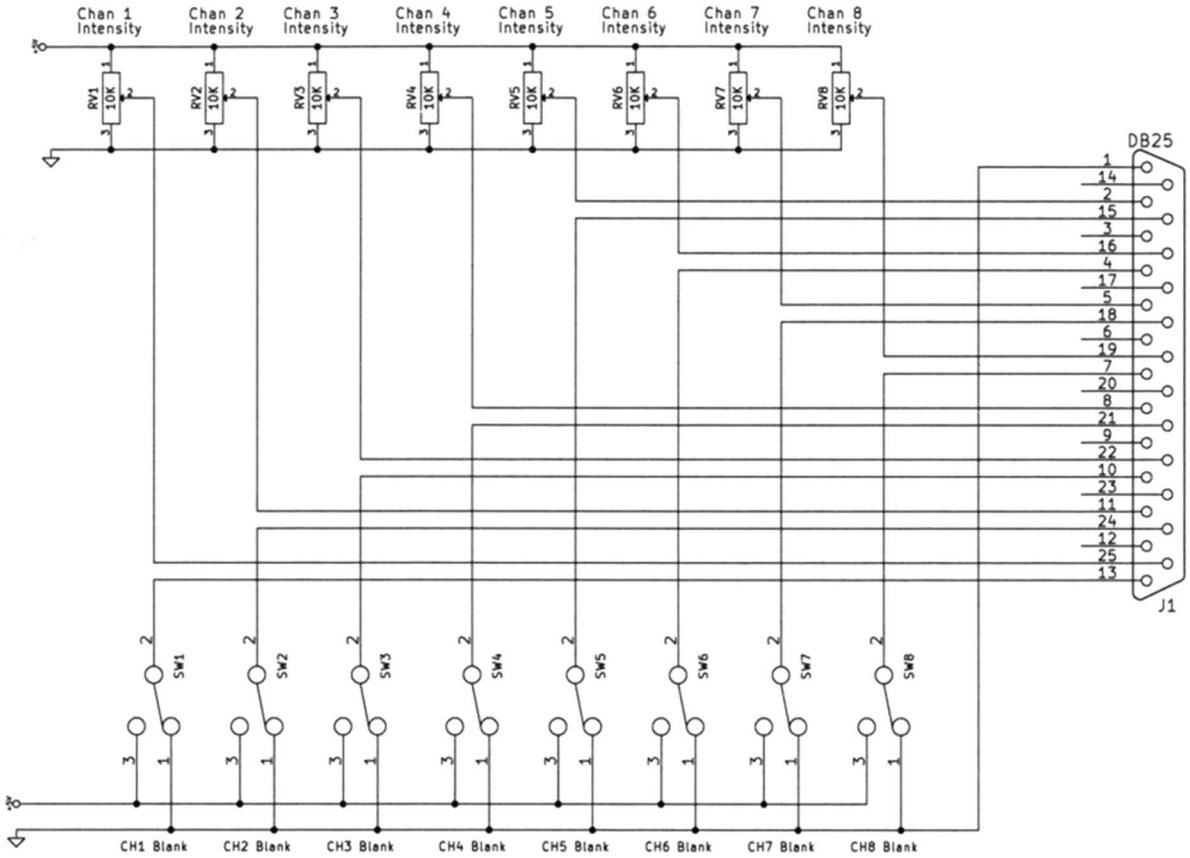

FIG. 4. Schematic diagram of the analog manual controller. A 5 V dc power supply is connected to 10 kΩ variable resistors that control the RF signal amplitude and hence the laser intensity of the respective wavelength. The wiring for the parallel port interface corresponds to the pin-assignment of the AOTF driver unit. The switches on each line can either turn the laser on/off or be placed in remote control position.

to separate the fluorescence into the two and four spectral channels in the Dualview and Quadview, respectively, are listed in Table II. The multi-band mirrors for the lasers used inside the turret in conjunction with the Quadview and Dualview for performing multi-color FRET measurements are listed in Table III. The individual exciters and emitters in the Sedat filter sets (Semrock) are placed in the motorized excitation and emission filter wheels, respectively. Table IV shows the measurements of the output power of the different laser wavelengths at the optic fibers and the microscope objective and the respective telescope magnification.

TABLE I. The list of the epifluorescence filter sets for the two microscopes and the fluorophores used with the respective filter set.

Bright field filters	Fluorophores	Quantity
DAPI-5060B-000-Zero	DAPI, Alexa Fluor 405, BFP	2
CFP-2432A-000-Zero	CFP, ECFP, BOBO-1	1
FITC-3540B	FITC, Alexa Fluor 488, Bodipy 505	2
GFP-3035B-000-Zero	GFP, Cy2, YOYO-1	1
YFP-2427A-000-Zero	YFP, Rhodamine Green	1
Cy3-4040B-000-Zero	Cy3, TAMRA, Alexa Fluor 555, DsRed	2
mCherry-A-000-Zero	mCherry	1
Cy5-4040A-000-Zero	Cy5, Alexa Fluor 647, Alexa Fluor 660	2
Cy7-A-000-Zero	Cy7, Alexa Fluor 750	1
QD525-A-000	Qdot 525	1
QD655-A-000	Qdot 655	1
QDLP-A-000 Set	Qdot 705	1

[a]Alexa Fluor®Dyes, BOBO™-1, Biodipy Dyes, Qdot®, YOYO®-1 from Invitrogen.
[b]Cyanine dyes (Cy2–Cy7) GE Healthcare.

III. EXPERIMENT

In this section, we test the performance of the new setup by conducting a two-color alternating excitation (ALEX) single-molecule FRET experiment and a more technically challenging four-color single-molecule FRET experiment. The ability of FRET to measure distances in the nanometer scale makes it a powerful experimental approach to study biomolecular dynamics.[17] The two-color ALEX FRET measurements were made on double-stranded DNA (dsDNA) that has a pair of fluorophores, Cy3 (donor) and Cy5 (acceptor), situated nine and eighteen base pairs (bp) apart. The 9 bp dsDNA was prepared by annealing single-stranded DNA (ssDNA) oligonucleotides 5′-Biotin-TGGCGACGG-Cy5-3′ and 5′-CCGTCGCCA-Cy3-3′. The 18 bp dsDNA was prepared by annealing oligonucleotides 5′-Biotin-TGGCGACGGCAGCGAGGC-Cy5-3′ and 5′-GCCT-CGCTGCCGTCGCCA-Cy3-3′. The oligonucleotides were purchased from (Integrated DNA Technologies) and annealed in buffer containing 10 mM Tris-HCl (*p*H 8) and 50 mM NaCl, where the samples were heated to 95°C for 5 min and left to cool down slowly to room temperature. The experiment is performed in a microfluidic flow cell. The flow cell

Downloaded 28 Jun 2013 to 141.211.173.82. This article is copyrighted as indicated in the abstract. Reuse of AIP content is subject to the terms at: http://rsi.aip.org/about/rights_and_permissions

TABLE II. The list of the fluorophore combinations and the configuration of the two Dualview and the Quadview devices.

Description	Part number	Quantity
Dualview	DV2	2
Cube for (BFP/GFP) (Cyan and yellow emission)	DV2-505 cube	1
BFP emission filter	HQ440/40M-25	1
GFP emission filter	HQ535/40M-25	1
Cube for (FITC/Cy3) and (CFP/YFP) (green and red emission)	DV2-565 cube	1
FITC emission filter	HQ510/20M-25	1
Cy3 emission filter	HQ600/40M-25	1
CFP emission filter	HQ485/30M-25	1
YFP emission filter	HQ550/30M-25	1
Cube for (Cy3/Cy5), (GFP/RFP) and (FITC/Cy5)	DV2 filter cube	2
Dichroic for DV2 filter cube	630dcxr-18x26	2
Cy3 emission filter	HQ600/40M-25	2
Cy5 emission filter	HQ700/60M-25	2
GFP emission filter	HQ525/30M-25	1
RFP emission filter	HQ650/75M-25	1
Cy5 emission filter	HQ700/40M-25	1
Quadview 2	MSMI-QV	1
Cube for (DAPI/FITC/Cy3/Cy5)	QV-CUBE-SQ	1
Dichroic for QV filter cube	485dcxr-12-AR	1
Dichroic for QV filter cube	535dcxr-12-AR	1
Dichroic for QV filter cube	630dxcr-12-AR	1
DAPI emission filter	HQ440/40M-25	1
FITC emission filter	HQ510/20M-25	1
Cy3 emission filter	HQ600/40M-25	1
Cy5 emission filter	HQ700/60M-25	1
Cube for (CFP/YFP/RFP/DIC)	QV-CUBE-SQ	1
Dichroic for QV filter cube	510dcxr-12-AR	1
Dichroic for QV filter cube	565dcxr-12-AR	1
Dichroic for QV filter cube	630dxcr-12-AR	1
CFP emission filter	HQ485/30M-25	1
YFP emission filter	HQ535/20M-25	1
RFP emission filter	HQ600/50M-25	1
DIC emission filter	HQ715/60M-25	1

is constructed from a quartz slide with both inlet and outlet channels and a cover slip (No. 1 1/2) that are spaced by 100 μm thick polyethylene double-sided spacer SA-S-1L (Grace Biolabs). The surface of the cover slip is passivated and functionalized with a 1:100 ratio of biotinylated polyethylene glycol (Biotin-PEG-SVA MW 5,000) and polyethylene glycol (mPEG-SVA MW 5000) from Laysan Bio Inc.[18] The functionalized surface of the cover slip is then incubated for 30 min with 25 μl of (1 mg/ml) streptavidin (Sigma-Aldrich, S4762) dissolved in phosphate buffered saline diluted with the addition of 100 μl of a blocking buffer made of (20 mM Tris-HCl (*p*H 8), 2 mM EDTA, 50 mM NaCl, 0.2 mg/ml BSA, and 0.005% Tween 20). The flow cell is then washed with blocking buffer in order to remove the free streptavidin. This is followed by flowing the biotinylated dsDNA (100 pM) to bind to the surface immobilized streptavidin in O_2 scavenging buffer (described below), which is used to reduce molecular oxygen and to prolong the observation of fluorescence emission signal. O_2 scavenging system minimizes intensity fluctuations on the millisecond timescale (blinking) and fast photobleaching as a result of the conversion of the excited states to transient or permanent dark states, respectively. We employ enzymatic oxygen scavenging system based on protocatechuic acid (PCA) 6 mM (Sigma-Aldrich, P5630) and protocatechuate-3,4-dioxygenase (PCD) 60 nM (Sigma-Aldrich, P8279-25UN), which significantly improves the stability of Cy3 and Cy5 dyes. Trolox at concentration of 2 mM is added as a triplet-state quencher (Acros Organics 21894).[17] The Cy3 and Cy5 were excited with 532 and 640 nm, respectively, where the lasers are reflected off the surface of a dual-band dichroic FF560/659-Di01-25×36 (Semrock) and focused through 100× Napo oil-immersion objective at fluence 180 W/cm^2. The emissions of the donor and the acceptor are split inside the Dualview by 630dcxr-18×26 dichroic (Chroma Inc.), where the shorter wavelength (donor emission) and longer wavelength (acceptor emission) pass through HQ580/40-P and HQ680/40 filters (Chroma Inc.), respectively. The images of the surface-immobilized molecules were recorded by alternating green (532 nm) and red (640 nm) wavelengths. The image acquisition was synchronized to the laser excitation through triggering the AOTF by the EMCCD camera to prevent the photobleaching of the sample when images are not being acquired. The Dualview images of the 18 bp dsDNA resulting from the green and red excitations are shown in Figures 5(a) and 5(b), respectively. The image is split into two identical halves; the left and right channels are the emissions of Cy3 and Cy5, respectively. Mapping the donor and the acceptor channels is performed by imaging a diluted sample of fluorescent beads (FluoSpheres, F8810 Invitrogen) in TIRF mode. Only molecules detected in both emission channels, i.e., have single donor and acceptor pair, are analyzed. Molecules that are too dim or too bright or very close to each other are excluded from the analysis to minimize errors. The photon counts are measured from the molecular point-spread functions (PSFs) in the donor and acceptor emission channels, by fitting the molecular PSFs with a two-dimensional Gaussian and calculating the apparent FRET efficiency.[19] The two-color alternating excitation of both the donor and acceptor provides two ratios: the first is the stoichiometry-based ratio (S), a parameter that is sensitive to the stoichiometry of donor and acceptor and their relative brightness and the second is the intramolecular distance-dependent ratio FRET efficiency (E). S is distance-independent and assumes intermediate values for molecules containing both donor and acceptor, whereas S for molecules containing acceptor-only species is close to 0 and for molecules with donor-only species is close to 1.[20] The two-dimensional histograms of E and S and the individual E and S histograms for the 9 and 18 bp two-color ALEX are depicted in Figures 5(c) and 5(d), respectively. The 9 bp dsDNA molecules exhibit a high FRET E (upper histogram) and correlates with S histogram (right) at S centered around 0.6 (Figure 5(c)). The 18 bp dsDNA molecules show a medium FRET E and correlates with S histogram at S centered around 0.7 (Figure 5(d)). The FRET values for the 18 and 9 bp constructs agree with their expected theoretical distances.

Fast alternation in laser excitation provides accurate stoichiometry and measurements of multiple FRET efficiencies in real time.[21,22] Alternating excitation with three

Downloaded 28 Jun 2013 to 141.211.173.82. This article is copyrighted as indicated in the abstract. Reuse of AIP content is subject to the terms at: http://rsi.aip.org/about/rights_and_permissions

TABLE III. The list of the multi-band mirrors for single-molecule FRET inside the turret that are used in conjunction with the Quadview and Dualview devices and the respective fluorophores.

Multi-band mirrors	Fluorophores	Intended use	Quantity
Z405/488/640rpc	FITC/Cy5	Dualview, two-color FRET and photoswitchable proteins	2
	PA-GFP[a]/Cy5		
	Dronpa[a]/Cy5		
Z405/488/532/640rpc	(DAPI/FITC/Cy3/Cy5)	Quadview, four-color FRET and photoswitchable proteins	2
Z457/514rpc	(CFP/YFP)	Dualview, two-color FRET	2
Z532/640rpc	(Cy3/Cy5)	Dualview, two-color FRET	2
Z457/514/561/640rpc	CFP/YFP/Cy5	Quadview, three-color FRET	1
Z405/488/561rpc	FITC/PhotoswitchableEosFP[a]	Dualview, photoswitchable proteins	1
Sedat laser filter set DAPI/FITC/mCherry/Cy5 optimized for 405/488/561/635 nm	LF405/488/561/635-4X4M-A-000 Includes Quad-band mirror Di01-R405/488/561/635-25x36 Quad-band emission filter FF01-446/523/600/677-25	Quadview, four-color FRET single-band exciters and single and quad band emitters in the excitation and emission filter wheels	2
Sedat laser filter set Cy3/Cy5	Cy3/Cy5-2X2M-A	Dualview, two-color FRET single-band exciter and emitters in filter wheels	2
Filter set for TIRF 405 nm	Z410RDC, ET480/40M	Single-color TIRF	2
Filter set for TIRF 457 nm	Z458RDC, ET485/30M		1
Filter set for TIRF 488 nm	Z488RDC, ET525/50M		2
Filter set for TIRF 514 nm	Z514RDC, HQ545/30M		1
Filter set for TIRF 532 nm	Z532RDC, HQ545LP		2
Filter set for TIRF 561 nm	Z561RDC, ET605/70M		2
Filter set for TIRF 635 nm	Z633RDC, HQ675/55M		2

[a]The wavelengths used for photoactivation and excitation of photoswitchable proteins are underlined.

lasers has led to the development of three-color FRET experiments that were used to study the folding and cleavage rates of 8–17 deoxyribozyme,[23,24] the diffusion of ssDNA-binding protein,[25] dynamics of Holliday junction[26] and substrate translocation through the ribosome.[27] Recently, four-color FRET experiments on Holliday junction[13] and DNA origami[28] were achieved by alternating excitation with three lasers in a scheme that involves the direct excitation of three fluorophores in the visible region and measuring the FRET signal from the forth fluorophore in the near infrared region; either Cy7 or AlexaFlour 750 were used as the near infrared fluorophore due to their photostability and to achieve lower background.

In this study we perform, to our knowledge for the first time, alternating-laser excitation of four fluorophores with four different excitation colors in TIRF configuration, where one fluorophore is near the ultraviolet region and the other three are in the visible region. The sample is a Holliday junction that has four arms and carries four different fluorophores as depicted in Figure 6(a). The four fluorophores are three different Atto dyes®: Atto 425, 488, and 647 and Cy3 cyanine dye, both types of dyes have high photostability, distinct spectra and are suitable for single-molecule fluorescence measurements. The Holliday junction substrate was prepared by annealing equimolar amounts of the following four ssDNA oligo nucleotides purchased from (Eurofins

TABLE IV. The list of the measurements of the laser power outputs in milliwatts (mW) from the optic fibers and the microscope 100× objective.

	405		488		532		561		640	
Wavelength	1-line	4-line	1-line	4-line	1-line	4-line	1-line	4-line	1-line	4-line
Power at the objective 100% (mW)	2.8	2	17	7.4	16	11	14	9.4	18	13.2
Fiber output at 100% (mW)	17	11.5	31	20	28	26	25	35	31	28
Power at the objective at 50/50 beam splitting (mW)	1.7	0.9	7	4	7	5	10	4	9.5	5
Fiber output at 50/50 beam splitting (mW)	5	4	14	10	13	10	19	16	18	9
After 50/50 beam splitter (mW)	40.4	38	42	44.5	38	36	42	40	43	41
Telescope magnification	2×		2.77×		2.77×		2×		2×	
Laser source (mW)	90		106		117		105		112	

Downloaded 28 Jun 2013 to 141.211.173.82. This article is copyrighted as indicated in the abstract. Reuse of AIP content is subject to the terms at: http://rsi.aip.org/about/rights_and_permissions

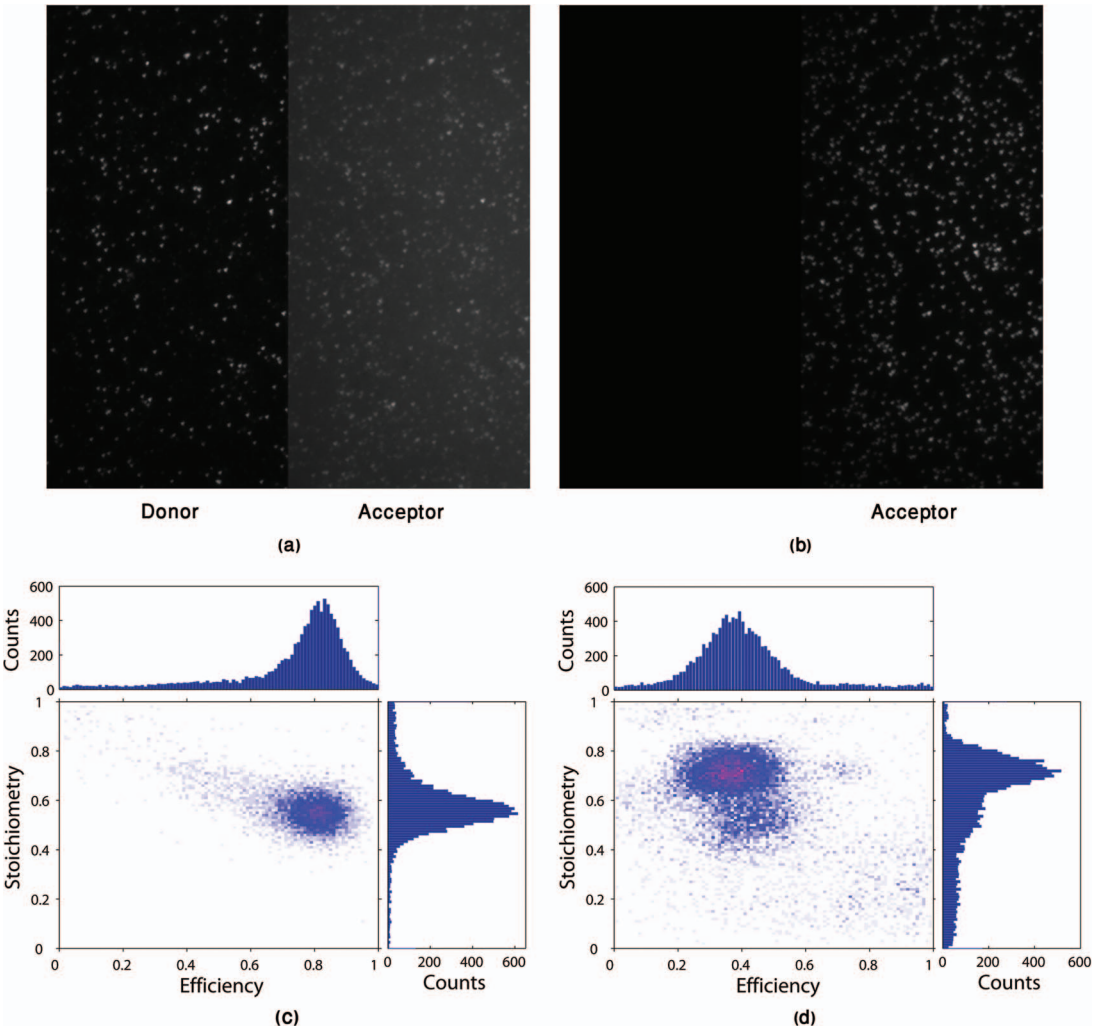

FIG. 5. (Color) (a) Dualview image of the surface-immobilized 18 bp dsDNA molecules excited with green laser (532 nm). The donor emission resulting from direct excitation, and acceptor emission resulting from FRET, appear on the left and right channels, respectively. (b) Dualview image of the excitation of the surface-immobilized DNA with red laser (640 nm). Only the acceptor molecules are excited. (c) The two-dimensional (2D) histograms of FRET Efficiency E and Stoichiometry S obtained from two-color ALEX measurement for the 9 bp dsDNA showing high E. (d) The 2D histograms of E and S for the 18 bp dsDNA showing medium E. S exhibit intermediate values for molecules with donor-acceptor.

MWG Operon) in 10 mM Tris-HCl (pH 8) and 100 mM NaCl:

b-strand 5′-Atto488-CCCTAGCAAGCCGCTGCTAC-GG-3′ (22 bp),
h-strand 5′-Cy3-CCGTAGCAGCGCGAGCGGTGGG-Atto425-3′ (22 bp),
r-strand 5′-Biotin-CCCACCGCTCGGCTCAACTGGG-Atto647-3′ (22 bp), and
x-strand 5′-GGGCGGCGACCTCCCAGTTGAGCGC-TTGCTAGGG-3′ (34 bp).

The sample was immobilized to the surface via biotin-streptavidin linkage and imaged in 10 mM Tris-HCl (pH 8), 100 mM $MgCl_2$ and O_2 scavenging solution as described above for the two-color ALEX FRET measurements. The emission is split by the Quadview into four spectral channels using 485dcxr-12-AR, 535dcxr-12-AR and 630dxcr-12-AR dichroics. The emission filters for the four channels of the Atto 425, Atto 488, Cy3, and Atto 647 (Cy5 equivalent) fluorophores are 1 in. diameter HQ440/40M, HQ510/20M, HQ600/40M, and HQ700/60M filters (Chroma Technologies Inc.), respectively. The acquisition of the four-channel images from the Quadview is synchronized to each of the four-excitation wavelengths. Figure 6(b) shows the average emission intensity of the raw images obtained from each channel as a result of multiple cycles of direct alternating excitation with four different lasers. Upon excitation with each wavelength, the FRET signals appear in the longer wavelength emission channels besides the emission from the direct excitation of the respective fluorophore (data not shown).

The analysis of the above four-color ALEX FRET measurement and its comparison with the current four-color FRET scheme, which uses near infrared dye,[13,28] is required to determine its feasibility as a new four-color FRET scheme and will be subject of future study if it is found to be suitable. Nevertheless, our four-color ALEX FRET experiment serves the purpose of demonstrating the ability of our instrument to perform highly sensitive and technically demanding multi-color single-molecule FRET measurements applicable for studying complex biomolecules.

Downloaded 28 Jun 2013 to 141.211.173.82. This article is copyrighted as indicated in the abstract. Reuse of AIP content is subject to the terms at: http://rsi.aip.org/about/rights_and_permissions

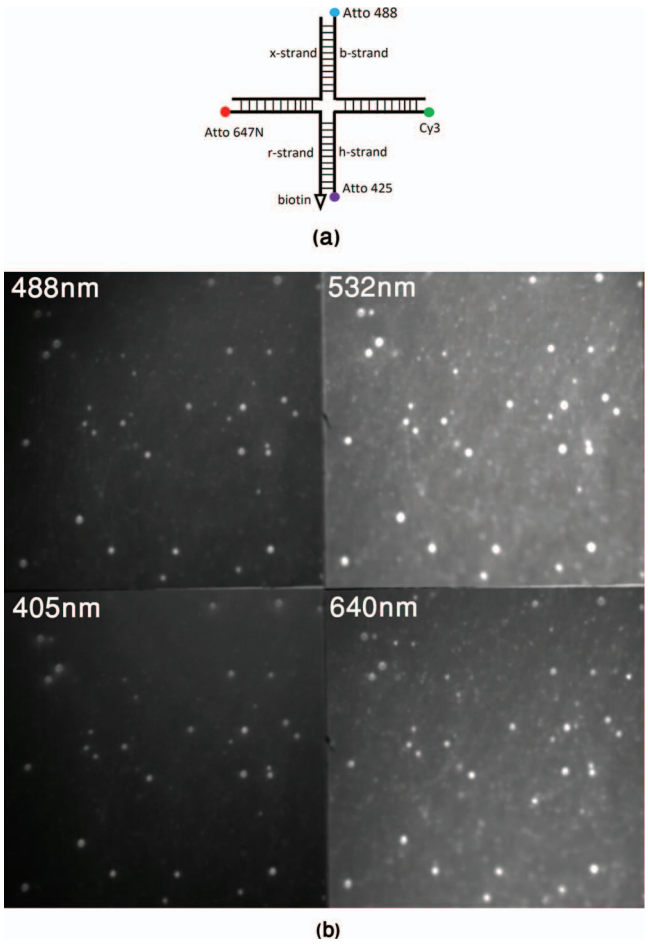

FIG. 6. (Color online) (a) Schematic of the Holliday junction construct. The four arms of the Holliday junction are labeled with four different fluorophores. (b) Raw images of the surface-immobilized Holliday junction molecules. The four-color FRET image shows the average of the fluorescence images from the alternate excitation with the 405, 488, 532, and 640 nm wavelengths.

IV. CONCLUSION

We have presented a detailed description of the design of a versatile single-molecule TIRF setup with multiple laser excitation and four-color detection that is well suited for multicolor FRET imaging and multi-color single-particle tracking. Although not demonstrated here, the setup can provide the necessary photoactivation and photoexcitation schemes required for super-resolution imaging. At the heart of the setup is the laser combiner module, which with its remotely controlled motorized components and AOTFs, makes it feasible and reproducible to program simultaneous and alternating excitation schemes with few microseconds switching time between multiple laser sources and in transparent and easy manner for the end user. The use of optic fibers provides excellent pointing stability and reproducibility. Coupling the lasers by individual fiber ports allows the accurate control of the incidence angle for each wavelength and equal penetration depth for the different wavelengths into the sample. The selected filter sets for the Dualview and Quadview devices are compatible with a wide selection of fluorophores and photoswitchable labels. We presented two and four-color ALEX FRET experiments on doubly labeled duplex DNA and quadruple-labeled Holliday junction, respectively. We aim to use this advanced single-molecule TIRF setup to study the biomolecular dynamics of the multi-protein DNA replication complexes, the replisome, and its interplay with other biological processes such as DNA repair and recombination.[29–33]

ACKNOWLEDGMENTS

M.S., M.E., M.T., and S.H. acknowledge the financial support from the Faculty Initiated Collaboration (FIC) Grant by King Abdullah University of Science and Technology.

[1] S. M. Hamdan and C. C. Richardson, Ann. Rev. Biochem. **78**, 205 (2009).
[2] *Single-molecule Techniques: A Laboratory Manual*, edited by P. R. Selvin and T. Ha, (Cold Spring Harbor Laboratory Press, New York, 2008).
[3] N. G. Walter, C. Huang, A. J. Manzo, and M. A. Sobhy, Nat. Methods **5**, 475 (2008).
[4] C. Bustamante, Annu. Rev. Biochem. **77**, 45 (2008).
[5] D. Axelrod, Traffic **2**, 764 (2001).
[6] T. Ha, T. Enderle, D. F. Ogletree, D. S. Chemla, P. R. Selvin, and S. Weiss, Proc. Natl. Acad. Sci. U.S.A. **93**, 6264 (1996).
[7] R. Roy, S. Hohng, and T. Ha, Nat. Methods **5**, 507 (2008).
[8] C. Joo, H. Balci, Y. Ishitsuka, C. Buranachai, and T. Ha, Ann. Rev. Biochem. **77**, 51 (2008).
[9] A. Jain, R. Liu, B. Ramani, E. Arauz, Y. Ishitsuka, K. Ragunathan, J. Park, J. Chen, Y. K. Xiang, and T. Ha, Nature **473**, 484 (2011).
[10] A. Sharonov and R. M. Hochstrasser, Proc. Natl. Acad. Sci. U.S.A. **103**, 18911 (2006).
[11] S. Hohng, C. Joo, and T. Ha, Biophys. J. **87**, 1328 (2004).
[12] M. Bates, B. Huang, and X. Zhuang, Curr. Opin. Chem. Biol. **12**, 505 (2008).
[13] J. Lee, S. Lee, K. Ragunathan, C. Joo, T. Ha, and S. Hohng, Angew. Chem. Int. Ed. **49**, 9922 (2010).
[14] E. Betzig, G. H. Patterson, R. Sougrat, O. W. Lindwasser, S. Olenych, J. S. Bonifacino, M. W. Davidson, J. Lippincott-Schwartz, and H. F. Hess, Science **313**, 1642 (2006).
[15] S. T. Hess, T. P. K. Girirajan, and M. D. Mason, Biophys. J. **91**, 4258 (2006).
[16] M. J. Rust, M. Bates, and X. W. Zhuang, Nat. Methods **3**, 793 (2006).
[17] C. E. Aitken, R. A. Marshall, and J. D. Puglisi, Biophys. J. **94**, 1826 (2008).
[18] T. Ha, I. Rasnik, W. Cheng, H. P. Babcock, G. Gauss, T. M. Lohman, and S. Chu, Nature **419**, 638 (2002).
[19] S. J. Holden, S. Uphoff, J. Hohlbein, D. Yadin, L. Le Reste, O. J. Britton, and A. N. Kapanidis, Biophys. J. **99**, 3102 (2010).
[20] A. N. Kapanidis, N. K. Lee, T. Laurence, S. Doose, E. Margeat, and S. Weiss, Proc. Natl. Acad. Sci. U.S.A. **101**, 8936 (2004).
[21] N. K. Lee, A. N. Kapanidis, Y. Wang, X. Michalet, J. Mukhopadhyay, R. H. Ebright, and S. Weiss, Biophys. J. **88**, 2939 (2005).
[22] N. K. Lee, A. N. Kapanidis, H. R. Koh, Y. Wang, S. O. Ho, Y. Kim, N. Gassman, S. K. Kim, and S. Weiss, Biophys. J. **92**, 303 (2007).
[23] N. K. Lee, H. R. Koh, K. Y. Han, and S. K. Kim, J. Am. Chem. Soc. **129**, 15526 (2007).
[24] N. K. Lee, H. R. Koh, K. Y. Han, J. Lee, and S. K. Kim, Chem. Commun. **46**, 4683 (2010).
[25] R. Roy, A. G. Kozlov, T. M. Lohman, and T. Ha, Nature **461**, 1092 (2009).
[26] S. Lee, J. Lee, and S. Hohng, PLoS ONE **5**, e12270 (2010).
[27] J. B. Munro, R. B. Altman, C. Tung, J. H. D. Cate, K. Y. Sanbonmatsu, and S. C. Blanchard, Proc. Natl. Acad. Sci. U.S.A. **107**, 709 (2010).
[28] I. H. Stein, C. Steinhauer, and P. Tinnefeld, J. Am. Chem. Soc. **133**, 4193 (2011).
[29] S. M. Hamdan, J. J. Loparo, M. Takahashi, C. C. Richardson, and A. M. van Oijen, Nature **457**, 336 (2009).
[30] S. M. Hamdan, D. E. Johnson, N. A. Tanner, J.-B. Lee, U. Qimron, S. Tabor, A. M. van Oijen, and C. C. Richardson, Mol. Cell **27**, 539 (2007).
[31] N. A. Tanner, S. M. Hamdan, S. Jergic, K. V. Loscha, P. M. Schaeffer, N. E. Dixon, and A. M. van Oijen, Nat. Struct. Mol. Biol. **15**, 170 (2008).
[32] N. A. Tanner, J. J. Loparo, S. M. Hamdan, S. Jergic, N. E. Dixon, and A. M. van Oijen, Nucleic Acids Res. **37**, e27 (2009).
[33] C. M. Etson, S. M. Hamdan, C. C. Richardson, and A. M. van Oijen, Proc. Natl. Acad. Sci. U.S.A. **107**, 1900 (2010).

Downloaded 28 Jun 2013 to 141.211.173.82. This article is copyrighted as indicated in the abstract. Reuse of AIP content is subject to the terms at: http://rsi.aip.org/about/rights_and_permissions